Evidence for ferromagnetic coupling at the doped topological insulator/ferrimagnetic insulator interface

Wenqing Liu,[1,2,3,a] Liang He,[2,a] Yan Zhou,[2,3] Koichi Murata,[4] Mehmet C. Onbasli,[5] Caroline A. Ross,[5] Ying Jiang,[6] Yong Wang,[6] Yongbing Xu,[1,2,b] Rong Zhang,[2,b] and Kang. L. Wang[4,b]

[1]*Spintronics and Nanodevice Laboratory, Department of Electronics, University of York, York YO10 5DD, United Kingdom*
[2]*York-Nanjing Joint Centre for Spintronics and Nano Engineering (YNJC), School of Electronics Science and Engineering, Nanjing University, Nanjing 210093, China*
[3]*Physics Department, Hong Kong University, Hong Kong*
[4]*Department of Electrical Engineering, University of California, Los Angeles, California 90095, USA*
[5]*Department of Materials Science and Engineering, Massachusetts Institute of Technology, Cambridge, Massachusetts 02139, USA*
[6]*Centre of Electron Microscopy, State Key Laboratory of Silicon Materials, Department of Materials Science and Engineering, Zhejiang University, Hangzhou, 310027, China*

(Presented 15 January 2016; received 6 November 2015; accepted 11 December 2015; published online 3 March 2016)

One of the major obstacles of the magnetic topological insulators (TIs) impeding their practical use is the low Curie temperature (T_c). Very recently, we have demonstrated the enhancement of the magnetic ordering in Cr-doped Bi_2Se_3 by means of proximity to the high-T_c ferrimagnetic insulator (FMI) $Y_3Fe_5O_{12}$ and found a large and rapidly decreasing penetration depth of the proximity effect, suggestive of a different carrier propagation process near the TI surface. Here we further present a study of the interfacial magnetic interaction of this TI/FMI heterostrucutre. The synchrotron-based X-ray magnetic circular dichroism (XMCD) technique was used to probe the nature of the exchange coupling of the $Bi_{2-x}Cr_xSe_3/Y_3Fe_5O_{12}$ interface. We found that the $Bi_{2-x}Cr_xSe_3$ grown on $Y_3Fe_5O_{12}(111)$ predominately contains Cr^{3+} cations, and the spin direction of the Cr^{3+} is aligned parallel to that of tetrahedral Fe^{3+} of the YIG, revealing a ferromagnetic exchange coupling between the $Bi_{2-x}Cr_xSe_3$ and the $Y_3Fe_5O_{12}$. [http://dx.doi.org/10.1063/1.4943157]

Three-dimensional (3D) TIs feature novel phases of quantum matter with an insulating bulk band gap and gapless Dirac-like band dispersion surface states (SS). Unlike the different electronic properties of the surface and the bulk universally existing in all solids owing to the inevitable termination of the periodic lattice structure near the surface, TIs present a new class of nontrivial SS arising from the intrinsic strong spin-orbital coupling.[1–3] These low-dimensional conducting states are immune to localization as long as the disorder potential is time-reversal-invariant[4] and therefore have strong implications for emerging technologies such as dissipationless spintronics and quantum computing. Breaking time-reversal-invariance by introducing magnetic perturbation, on the other hand, reveals a complex phenomenology associated with an excitation gap of the surface spectrum, resembling that of a massive Dirac fermion.[5,6] Such a system with a tunable gap promises rich exotic topological phenomena and would allow purely electric control of the surface transport and magnetization.[7–10]

[a]Authors contributed equally to this work.
[b]Authors to whom correspondence should be addressed. Electronic addresses: yongbing.xu@york.ac.uk, rzhang@nju.edu.cn, and wang@seas.ucla.edu

Breaking TRS can be accomplished by either doping the TI host with magnetic ions or by designing TI/magnetic heterostructures.[11–32] Within the growing family of magnetically doped TIs, ferromagnetism has been observed in Cr- and Mn-doped single crystals of Sb_2Te_3,[11–13] Fe- and Mn-doped single crystals of Bi_2Te_3,[14,15] and Mn- and Cr-doped thin films of Bi_2Se_3.[16–18] Apart from transition metals, rare-earth metals such as Gd,[19] Dy, and Sm[20] have also been explored as an effective dopant to induce long-range magnetic ordering in Bi_2Se_3 or Bi_2Te_3.[21] Growing TIs on top of ferromagnetic metals (FMs) and insulators (FMIs), or vice versa, has been shown to produce an exchange interaction affecting the SS of TIs. Although pioneering theoretical work on TIs has demonstrated a pronounced effect of an adjacent magnetic layer,[22–24] successful experimental demonstrations are rather limited, and include that of GdN/Bi_2Se_3 by Kandala *et al.*,[25] and EuS/Bi_2Se_3 by Yang *et al.*,[26] and Wei *et al.*[27] Moreover the effect is limited to low temperature (< 22 K) due to the low T_C of the selected FMI. The interfacial magnetism of (anti-)FM/TI heterostructures, such as Fe/Bi_2Se_3,[28–30] Co/Bi_2Se_3[29] and Fe/$Bi_{2-x}Mn_xTe_3$[31] has also been investigated and robust magnetism was obtained by means of proximity effects. However, it should be noted that with the presence of a metallic layer, the SS of the TI can be significantly altered, and device designs are constrained due to the short circuit caused by the metal layer.

This work focusses on a heterostructure consisting of a magnetically-doped TI interfaced with a FMI. The T_c of the magnetically doped TIs, generally less than ~35 K, is still well below room temperature (RT).[11–20] However, very recently we published a work demonstrating enhancement of the magnetic ordering in Cr-doped Bi_2Se_3 grown on a ferrimagnetic insulator (FMI) $Y_3Fe_5O_{12}$ (YIG) via the proximity effect.[32] Garnet-type YIG is a well-known FMI with a high T_C (~550 K) and a long spin diffusion length. YIG is ferrimagnetic and each formula unit contains two Fe ions occupying octahedral sites and three Fe ions occupying tetrahedral sites coupled antiparallel. Proximity effects have been demonstrated in PdPt/YIG,[33] Pt/YIG,[34] and Nb/YIG.[35] Strong exchange coupling effects are anticipated in heterostructures consisting of materials with two-dimensional quantum surface states, as in our experimental system $Bi_{2-x}Cr_xSe_3/Y_3Fe_5O_{12}$.[32] This work demonstrated that the penetration depth of the proximity effect was large (up to 6 nm at 30 K) and decreased quickly with increasing temperature (by 80% from 30 to 50 K), compared to that of conventional dilute ferromagnetic semiconductors (DMSs), suggestive of a different mechanism for carrier propagation near the TI surface.[36] Here we present a further study of the interfacial magnetic interaction in this bilayer system using the synchrotron-based XMCD technique.[37–40] The unique elemental selectivity of XMCD enables unambiguous determination of the nature of magnetic coupling of the doped TI/FMI interface by measuring independently the magnetization of the doped TI and the YIG as a function of temperature.

Samples[32] consisted of 50 nm YIG (111) films, which were deposited on gallium gadolinium garnet ($Gd_3Ga_5O_{12}$ or GGG) (111) substrates using pulsed-laser deposition (PLD),[41,42] then coated with 10 nm $Bi_{1.89}Cr_{0.11}Se_3$ thin films grown at 200 °C in a Perkin-Elmer molecular-beam epitaxy (MBE) system. Structural and magnetic properties of YIG were measured by X-ray diffraction (XRD) and magneto-optical Kerr effect (MOKE) magnetometry as reported previously.[43] Bi (99.9999%) and Cr (99.99%) were evaporated from effusion cells at 470°C and Se (99.99%) from a cracker cell at 240 °C, and growth of the $Bi_2Cr_{2-x}Se_3$ was monitored by reflection high-energy electron diffraction (RHEED). Figure 1(a)-1(b) presents a typical RHEED pattern of the $Bi_{1.89}Cr_{0.11}Se_3$ epitaxial thin film grown on YIG(111) compared with that on Si(111). The diffraction patterns and in-plane lattice constants are similar suggesting that the enhancement of T_C for the $Bi_{1.89}Cr_{0.11}Se_3$/YIG, above that of of $Bi_{1.89}Cr_{0.11}Se_3$/Si (~20 K), is more likely due to the presence of the YIG than to structural changes caused by the substrates.

The detailed interfacial topography and crystalline structure were characterized using high-angle annular dark-field (HAADF) high-resolution scanning transmission electron microscopy (STEM). Cross-sectional foils of $Bi_{1.89}Cr_{0.11}Se_3$/YIG(111) and YIG/GGG(111) were prepared by focused ion beam (FIB), during which all parameters were carefully optimized to avoid ion injection and specimen damage, including the accelerating voltage, beam current, and tilt angle. As presented in Figure 2(a)-2(b), the HAADF images confirm the highly ordered hexagonal and

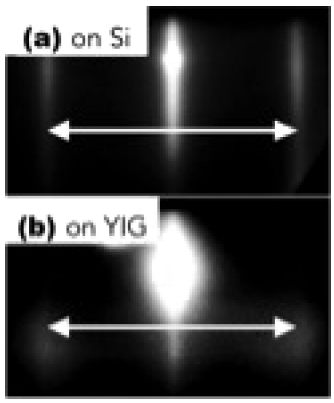

FIG. 1. RHEED characterization. Typical RHEED pattern of the $Bi_{1.89}Cr_{0.11}Se_3$ epitaxial thin film grown on (a) Si (111) and (b) YIG (111) substrates in the same MBE system. Arrows indicate the in-plane lattice constant.

quintuple-layered structure of the $Bi_{2-x}Cr_xSe_3$ thin films without detectable Cr segregation. Owing to the high stability of YIG and the relatively low growth temperature of $Bi_{1.89}Cr_{0.11}Se_3$, no significant intermixing occurs at the $Bi_{1.89}Cr_{0.11}Se_3$/YIG and YIG/GGG interfaces.

The $Bi_{1.89}Cr_{0.11}Se_3$/YIG (111) was characterized initially by 4-point magneto-transport measurements. The films were patterned into Hall bar devices by CHF_3 dry etching for 20 s and contacts were made from Ti 10nm/Au 100 nm (Figure 3(a)). An AC current of 0.05 - 0.1 μA at 1300 Hz was applied and the voltage drop across inner contacts was detected. Figure 3(b) shows the Hall resistance (R_{xy}) vs. perpendicular field and the anomalous Hall resistance (R_{AHE}) which was found from $R_{AHE} = R_{xy} - R_0 \cdot H$,[44] in which the latter term represents the ordinary Hall resistance. Figure 3(c) compares R_{AHE} of $Bi_{1.89}Cr_{0.11}Se_3$ on YIG and on Si., from which it is clear that the TI/YIG has a higher T_C than TI/Si by about 20K. A similar difference was found from the longitudinal resistance R_{xx}. Weak anti-localization (WAL) was found for TI/YIG at low temperatures and low fields, indicative of the gapped topological surface states below T_C.[12,17,45] Up to at least 50 K the valleys of the WAL cusp exhibited a shift as the scan direction of the field was reversed, with minimum resistance at the coercive field H_c.

The magnetic moment of the Cr and Fe was measured at 6 - 300 K by X-ray absorption spectroscopy (XAS) and XMCD at the $L_{2,3}$ absorption edges, as described in Ref. 32. Beamline I10 at Diamond Light Source, UK was used with circularly polarized X-rays at normal incidence, Figure 4(a). The XAS measurements used total-electron yield detection (TEY) and the XMCD was calculated as the difference between the XAS spectra, $\sigma^- - \sigma^+$, for opposite X-ray helicity at 10 kOe. Figure 4(b)-4(c) shows XAS and XMCD of the Cr and the Fe of TI/TIG. The Cr line was attributed to predominately Cr^{3+} cations by comparison with the line shape of $CdCr_2Se_4$[46] and $CrFe_2O_4$ spinels.[47] We conclude from the lineshape that Cr^{3+} is present in Bi sites in the lattice, consistent with transport data.[17]

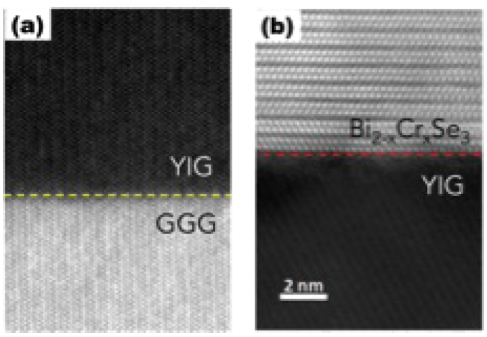

FIG. 2. HRTEM characterization. Cross-sectional HAADF-STEM image of (a) the $Bi_{1.89}Cr_{0.11}Se_3$/YIG and (b) the YIG/GGG interface. Dashed lines indicate the interfaces.

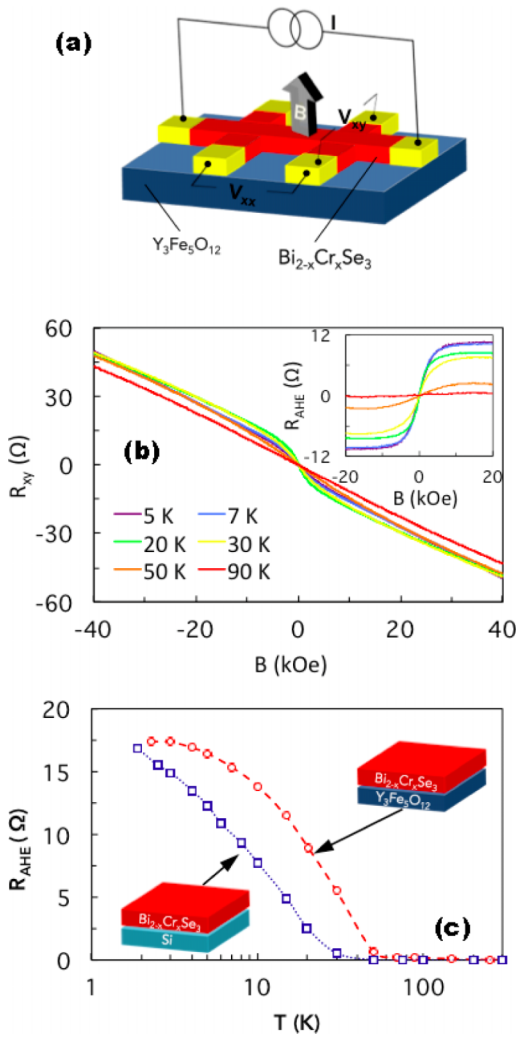

FIG. 3. Electrical-magneto-transport measurement. (a) Schematic diagram of the Hall bar device. (b) R_{xy} of the $Bi_{1.89}Cr_{0.11}Se_3$/YIG thin film versus magnetic field at 5 - 90 K. Inset shows R_{AHE} versus magnetic field. (c) A comparison of the R_{AHE} versus temperature of the $Bi_{1.89}Cr_{0.11}Se_3$ thin films grown on YIG (111) and Si (111), respectively (ref. 32).

On the other hand, the Fe XMCD shows a remarkably detailed multiplet structure and the XMCD spectrum shows alternating positive and negative peaks corresponding to the contributions of the octahedral Fe^{3+} and tetrahedral Fe^{3+} of YIG, respectively. The spin direction of the Cr^{3+} is aligned in parallel with that of tetrahedral Fe^{3+}, suggesting a ferromagnetic exchange interaction between the $Bi_{2-x}Cr_xSe_3$ and the YIG underlayer, as indicated by the sign of the XMCD spectra. Although no magnetic signature is distinguishable from the noise above 100 K for the $Bi_{1.89}Cr_{0.11}Se_3$, the YIG spectra remain strongly dichroic up to RT. The integration of the XMCD spectra or the summed peak intensity is a quantity proportional to the magnetic moment and here that of the Cr and Fe has the same sign. This means that unlike the antiphase proximity effect demonstrated by Vobornik *et al.*[48] with the $Bi_{2-x}Mn_xTe_3$/Fe system, in which the Mn and Fe are antiferromagnetically coupled, the net spin of the Fe and the Cr in the $Bi_{1.89}Cr_{0.11}Se_3$/YIG bilayer are aligned parallel, as schematically shown in Figure 4(d). Similar exchange coupling is present at the Co_2FeAl/(Ga, Mn)As interface.[36]

To summarize, we have studied the exchange interaction of the $Bi_{1.89}Cr_{0.11}Se_3$/YIG interface and provided direct evidence of ferromagnetic coupling in this technologically important TI/FMI bilayer system. The high quality $Bi_{1.94}Cr_{0.06}Se_3$/Si(111) epitaxial thin film was prepared using MBE, and characterized with STEM and magnetotransport measurements. The unique elemental

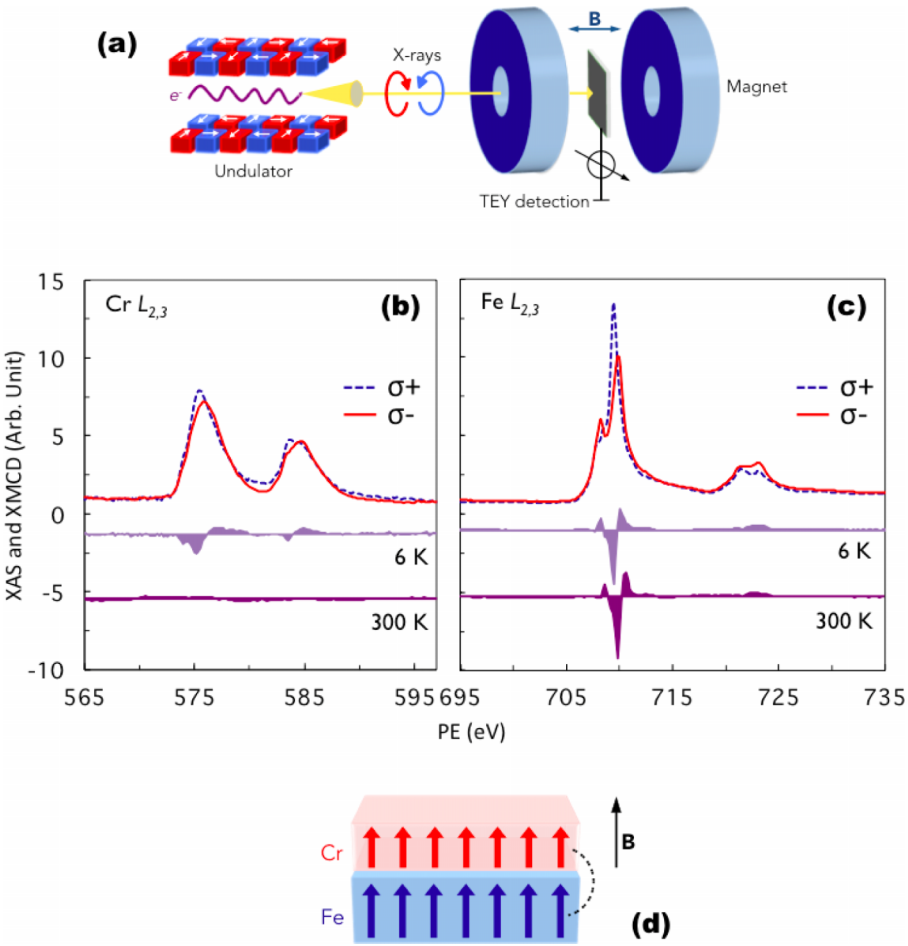

FIG. 4. XAS and XMCD measurement. (a) Schematic diagram of the experimental set up of the synchrotron-based XMCD experiment. Examples of XAS and XMCD spectra of (b) Cr and (c) Fe obtained at 6 K and 300 K, respectively. Data are offset for clarity. (d) Schematically illustration of the parallel alignment of the magnetic moment of the Cr and Fe of the $Bi_{2-x}Cr_xSe_3$/YIG heterostructure. The red and blue arrows represent the net spin of Cr and Fe, respectively. The magnetic field is applied perpendicular to the thin film plane.

selectivity of the XMCD technique enabled a direct determination of the relative magnetization of the Cr and the Fe. These results show that the Cr in the TI is coupled ferromagnetically with the net moment of the YIG, which is useful in stimulating experimental approaches to further increase the T_c in a magnetically doped TI via proximity effect. Future work to explore the tuning of the magnetization of TIs and its dependence on the band filling will have strong implications for both fundamental physics and emerging spintronics technology.

This work is supported by the State Key Programme for Basic Research of China (Grants No. 2014CB921101), NSFC (Grants No. 61274102), UK STFC, DARPA Meso program under contract No.N66001-12-1-4034 and N66001-11-1-4105. C. A. Ross and M. C. Onbasli acknowledge FAME, a STARnet Center of SRC supported by DARPA and MARCO, and the NSF. Diamond Light Source is acknowledged for beamtime on I10.

[1] G. Brumfiel, Nature **466**, 310 (2010).
[2] M.Z. Hasan and C.L. Kane, Rev. Mod. Phys. **82**, 3045 (2010).
[3] C.-X. Liu, X.-L. Qi, X. Dai, Z. Fang, and S.-C. Zhang, Phys. Rev. Lett. **101**, 146802 (2008).
[4] L. Fu, C.L. Kane, and E.J. Mele, Phys. Rev. Lett. **98**, 1 (2007).
[5] Y.L. Chen, J. Chu, J.G. Analytis, Z.K. Liu, K. Igarashi, H. Kuo, X.L. Qi, S.K. Mo, R.G. Moore, D.H. Lu, M. Hashimoto, T. Sasagawa, S.C. Zhang, I.R. Fisher, Z. Hussain, and Z.X. Shen, **329**, 659 (2010).

[6] L.A. Wray, S.-Y. Xu, Y. Xia, D. Hsieh, A. V. Fedorov, Y.S. Hor, R.J. Cava, A. Bansil, H. Lin, and M.Z. Hasan, Nat. Phys. **7**, 32 (2010).
[7] C.-Z. Chang, J. Zhang, X. Feng, J. Shen, Z. Zhang, M. Guo, K. Li, Y. Ou, P. Wei, L.-L. Wang, Z.-Q. Ji, Y. Feng, S. Ji, X. Chen, J. Jia, X. Dai, Z. Fang, S.-C. Zhang, K. He, Y. Wang, L. Lu, X.-C. Ma, and Q.-K. Xue, Science **340**, 167 (2013).
[8] I. Garate and M. Franz, Phys. Rev. Lett. **104**, 146802 (2010).
[9] T. Yokoyama, Y. Tanaka, and N. Nagaosa, Phys. Rev. B **81**, 121401 (2010).
[10] Y.Q. Zhang, N.Y. Sun, W.R. Che, X.L. Li, J.W. Zhang, R. Shan, Z.G. Zhu, and G. Su, Appl. Phys. Lett. **107**, 082404 (2015).
[11] J. Dyck, Č Drašar, P. Lošt'ák, and C. Uher, Phys. Rev. B **71**, 115214 (2005).
[12] Z. Zeng, T. a. Morgan, D. Fan, C. Li, Y. Hirono, X. Hu, Y. Zhao, J.S. Lee, J. Wang, Z.M. Wang, S. Yu, M.E. Hawkridge, M. Benamara, and G.J. Salamo, AIP Adv. **3**, 0 (2013).
[13] J. Dyck, P. Hájek, P. Lošt'ák, and C. Uher, Phys. Rev. B **65**, 115212 (2002).
[14] Y.S. Hor, P. Roushan, H. Beidenkopf, J. Seo, D. Qu, J.G. Checkelsky, L. a. Wray, D. Hsieh, Y. Xia, S.-Y. Xu, D. Qian, M.Z. Hasan, N.P. Ong, a. Yazdani, and R.J. Cava, Phys. Rev. B **81**, 195203 (2010).
[15] P.S. V.A. Kulbachinskii, A.Yu. Kaminskiia, K. Kindo, Y. Narumib, K. Sugab, and P. Lostak, Phys. B Condens. Matter **311**, 292 (2002).
[16] P.P.J. Haazen, J.-B. Laloë, T.J. Nummy, H.J.M. Swagten, P. Jarillo-Herrero, D. Heiman, and J.S. Moodera, Appl. Phys. Lett. **100**, 082404 (2012).
[17] L.J. Collins-McIntyre, M.D. Watson, a. a. Baker, S.L. Zhang, a. I. Coldea, S.E. Harrison, a. Pushp, a. J. Kellock, S.S.P. Parkin, G. van der Laan, and T. Hesjedal, AIP Adv. **4**, 127136 (2014).
[18] W. Liu, D. West, L. He, Y. Xu, J. Liu, K. Wang, and Y. Wang, ACS Nano **9**, 10237 (2015).
[19] Y.R. Song, F. Yang, M.-Y. Yao, F. Zhu, L. Miao, J.-P. Xu, M.-X. Wang, H. Li, X. Yao, F. Ji, S. Qiao, Z. Sun, G.B. Zhang, B. Gao, C. Liu, D. Qian, C.L. Gao, and J.-F. Jia, Appl. Phys. Lett. **100**, 242403 (2012).
[20] T. Chen, W. Liu, F. Zheng, M. Gao, X. Pan, G. Van Der Laan, X. Wang, Q. Zhang, F. Song, B. Wang, and B. Wang, Adv. Mater. (2015), DOI:10.1002/adma.201501254.
[21] S.E. Harrison, L.J. Collins-McIntyre, S.-L. Zhang, A.A. Baker, A.I. Figueroa, A.J. Kellock, A. Pushp, S.S.P. Parkin, J.S. Harris, G. van der Laan, and T. Hesjedal, J. Phys. Condens. Matter **27**, 245602 (2015).
[22] W. Luo and X.-L. Qi, Phys. Rev. B **87**, 085431 (2013).
[23] S. V. Eremeev, V.N. Men'shov, V. V. Tugushev, P.M. Echenique, and E. V. Chulkov, Phys. Rev. B **88**, 144430 (2013).
[24] V. Men'shov, V. Tugushev, S. Eremeev, P. Echenique, and E. Chulkov, Phys. Rev. B **88**, 224401 (2013).
[25] A. Kandala, A. Richardella, D.W. Rench, D.M. Zhang, T.C. Flanagan, and N. Samarth, Appl. Phys. Lett. **103**, 202409 (2013).
[26] Q.I. Yang, M. Dolev, L. Zhang, J. Zhao, A.D. Fried, E. Schemm, M. Liu, A. Palevski, A.F. Marshall, S.H. Risbud, and A. Kapitulnik, Phys. Rev. B **88**, 081407 (2013).
[27] P. Wei, F. Katmis, B. a. Assaf, H. Steinberg, P. Jarillo-Herrero, D. Heiman, and J.S. Moodera, Phys. Rev. Lett. **110**, 186807 (2013).
[28] L.A. Wray, S.-Y. Xu, Y. Xia, D. Hsieh, A. V. Fedorov, Y.S. Hor, R.J. Cava, A. Bansil, H. Lin, and M.Z. Hasan, Nat. Phys. **7**, 32 (2010).
[29] J. Li, Z.Y. Wang, A. Tan, P. -a. Glans, E. Arenholz, C. Hwang, J. Shi, and Z.Q. Qiu, Phys. Rev. B **86**, 054430 (2012).
[30] D. West, Y.Y. Sun, S.B. Zhang, T. Zhang, X. Ma, P. Cheng, Y.Y. Zhang, X. Chen, J.F. Jia, and Q.K. Xue, Phys. Rev. B **85**, 081305 (2012).
[31] I. Vobornik, U. Manju, J. Fujii, F. Borgatti, P. Torelli, D. Krizmancic, Y.S. Hor, R.J. Cava, and G. Panaccione, Nano Lett. **11**, 4079 (2011).
[32] W. Liu, L. He, Y. Xu, K. Murata, M.C. Onbasli, M. Lang, N.J. Maltby, S. Li, X. Wang, C. A. Ross, P. Bencok, G. van der Laan, R. Zhang, and K.L. Wang, Nano Lett. **15**, 764 (2015).
[33] X. Zhou, L. Ma, Z. Shi, G.Y. Guo, J. Hu, R.Q. Wu, and S.M. Zhou, Appl. Phys. Lett. **105**, 012408 (2014).
[34] Y. Lu, Y. Choi, C. Ortega, and X. Cheng, Phys. Rev. Lett. **147207**, 1 (2013).
[35] Z. Yang and V. V. Moshchalkov, J. Appl. Phys. **109**, 083908 (2011).
[36] S.H. Nie, Y.Y. Chin, W.Q. Liu, J.C. Tung, J. Lu, H.J. Lin, G.Y. Guo, K.K. Meng, L. Chen, L.J. Zhu, D. Pan, C.T. Chen, Y.B. Xu, W.S. Yan, and J.H. Zhao, Phys. Rev. Lett. **111**, 027203 (2013).
[37] G. van der Laan and A.I. Figueroa, Coord. Chem. Rev. **277–278**, 95 (2014).
[38] W.Q. Liu, Y.B. Xu, P.K.J. Wong, N.J. Maltby, S.P. Li, X.F. Wang, J. Du, B. You, J. Wu, P. Bencok, and R. Zhang, Appl. Phys. Lett. **104**, 142407 (2014).
[39] W.Q. Liu, M.Y. Song, N.J. Maltby, S.P. Li, J.G. Lin, M.G. Samant, S.S.P. Parkin, P. Bencok, P. Steadman, A. Dobrynin, Y.B. Xu, R. Zhang, D.L. Source, and D. Ox, J. Appl. Phys. **117**, 17E121 (2015).
[40] W.Q. Liu, W.Y. Wang, J.J. Wang, F.Q. Wang, C. Lu, F. Jin, a. Zhang, Q.M. Zhang, G. Van Der Laan, Y.B. Xu, Q.X. Li, and R. Zhang, Sci. Rep. **5**, 11911 (2015).
[41] T. Goto, M.C. Onbaşlı, and C. A. Ross, Opt. Express **20**, 28507 (2012).
[42] Y. Sun, Y.-Y. Song, H. Chang, M. Kabatek, M. Jantz, W. Schneider, M. Wu, H. Schultheiss, and A. Hoffmann, Appl. Phys. Lett. **101**, 152405 (2012).
[43] M. Lang, M. Montazeri, M.C. Onbasli, X. Kou, Y. Fan, P. Upadhyaya, K. Yao, F. Liu, Y. Jiang, W. Jiang, K.L. Wong, G. Yu, J. Tang, T. Nie, L. He, R.N. Schwartz, Y. Wang, C. a Ross, and K.L. Wang, Nano Lett. **14**, 3459–3465 (2014).
[44] N. Nagaosa, J. Sinova, S. Onoda, a. H. MacDonald, and N.P. Ong, Rev. Mod. Phys. **82**, 1539 (2010).
[45] M. Liu, J. Zhang, C.-Z. Chang, Z. Zhang, X. Feng, K. Li, K. He, L. Wang, X. Chen, X. Dai, Z. Fang, Q.-K. Xue, X. Ma, and Y. Wang, Phys. Rev. Lett. **108**, 036805 (2012).
[46] A. Kimura, J. Matsuno, J. Okabayashi, a. Fujimori, T. Shishidou, E. Kulatov, and T. Kanomata, Phys. Rev. B **63**, 224420 (2001).
[47] M. MIZUMAKI, A. AGUI, Y. SAITOH, M. NAKAZAWA, T. MATSUSHITA, and A. KOTANI, Surf. Rev. Lett. **09**, 849 (2002).
[48] I. Vobornik *et al.*, Nano Lett. **11**, 4079 (2011).